1-Benzyl-3,3,5′,6′-tetramethylspiro[indoline-2,2′-[2*H*]pyrano[3,2-*b*]-pyridinium] iodide, its hydrate, and a neutral precursor of the salts: synthesis, crystal structure, photochromic transformations in solutions and in crystals

E. A. Yurieva, S. M. Aldoshin, L. A. Nikonova, G. V. Shilov, and V. A. Nadtochenko*

Institute of Problems of Chemical Physics, Russian Academy of Sciences, 1 prosp. Akad. Semenova, 142432 Chernogolovka, Moscow Region, Russian Federation. E-mail: yurieva@icp.ac.ru

A new 1-benzyl-3,3,5′,6′-tetramethylspiro[indoline-2,2′-[2*H*]pyrano[3,2-*b*]pyridinium] iodide, photochromic in the crystal state, was obtained. X-ray diffraction analysis was used for determination of crystal structures of the salt, its hydrate, and a neutral precursor. It was found that a replacement of the substituent in the indoline fragment leads to a considerable change in the crystal structure of both the neutral spiropyran and the salts as compared to the analogs studied earlier. Effects of crystal structure on photochromic properties were studied.

Key words: spiropyrans, crystal structure, photochemistry in the crystal state.

Synthesis of photomagnets occupies an important place in the rapidly developing field of studies on creation of modern polyfunctional materials for electronics.[1—3] One of the approaches to the preparation of photomagnetic materials consists in the incorporation of photochromic organic molecules into the interlayer space of layered magnets, for example, layered copper(II)[4] and cobalt(II)[5] bihydroxides, bimetallic compounds with oxalate[6—8] or dithiooxalate[9—11] bridged bonds, *etc.*[12,13] In fact, the structural rearrangement and redistribution of electron density during isomerization of a photochromic molecule placed between magnetic layers open the way to the photocontrol of magnetic properties of a hybrid compound.

Representatives of three major classes of photochroms have been already used as photosensors in the hybrids based on layered magnets, they are azobenzene[4] and diarylethene[5,13] derivatives, as well as spiropyrans.[6—12] Among the photochromes that studied, cations of spiropyrans of the indoline series still remain the best photoswitches of magnetic properties for such hybrids.

In 2000, the spiro[indoline-pyranopyridinium] salts $(R—SP)^+I^-$ (Scheme 1) were described,[14] which exhibited photochromic properties in both solutions and crystals, and soon they were used for the synthesis of polyfunctional compounds.

The prospects in the use of spiropyran salts for preparation of polyfunctional compounds, as well as their unique photochemical properties in crystals stimulated further studies of these compounds.[15—19]

Scheme 1

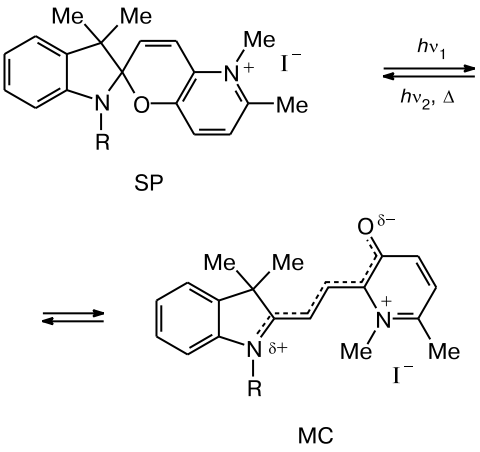

SP is the cyclic form, MC is the open (merocyanine) form

Earlier, while crystal structures of various salts $(R—SP)^+I^-$ were studied it was shown that photochromic transformations of $(R—SP)^+$ are due to the specific structure of the salt[15—18] and a dependence between the crystal packing density and the rate of the dark bleaching of the cation MC-form in these salts was established.[17]

In continuation of these systematic studies, we synthesized 1-benzyl-3,3,5′,6′-tetramethylspiro[indoline-2,2′-[2*H*]pyrano[3,2-*b*]pyridinium] iodide (**1**), studied crystal structures of the salt, its hydrate $\mathbf{1} \cdot H_2O$, and their

Published in Russian in *Izvestiya Akademii Nauk. Seriya Khimicheskaya,* No. 7, pp. 1379—1385, July, 2011.

1066-5285/11/6007-1401

neutral precursor **2**, as well as photochemistry of these compounds in solutions and crystals.

Experimental

2,3,3-Trimethylindolenine, benzyl bromide, and methyl iodide from Aldrich were used for the syntheses. 3-Hydroxy-6-methyl-2-pyridinecarbaldehyde (**3**) was obtained from furfurylamine (Aldrich) using the known procedures.[20,21] ^{1}H NMR spectra were recorded on a Bruker Avance 200 (200 MHz) spectrometer in $CDCl_3$ using Me_4Si as an internal standard.

1-Benzyl-3,3-dimethyl-2-methyleneindoline (4) was synthesized according to the modified method described earlier,[22] with the difference that the reaction of benzyl bromide with 2,3,3-trimethylindolenine was carried out in a homogeneous system using acetonitrile as a solvent instead of toluene. The residue after evaporation of acetonitrile was dissolved in diethyl ether, treated with 30% aqueous KOH, and compound **4** was isolated from the ethereal solution by distillation as a rapidly crystallized oil (b.p. 130—132 °C (0.2 Torr)).[22] Colorless crystals **4** (m.p. 63 °C) turn pink in air. Found (%): C, 86.62; H, 7.81; N, 5.77. $C_{18}H_{19}N$. Calculated (%): C, 86.70; H, 7.68; N, 5.62. ^{1}H NMR, δ: 1.43 (s, 6 H, Me); 3.89 (s, 2 H, C_{sp^3}=CH_2); 4.74 (s, 2 H, NCH_2); 6.53—7.36 (m, 9 H, Ar).

1-Benzyl-3,3,6′-trimethylspiro[indoline-2,2′-[2*H*]pyrano-[3,2-*b*]pyridine] (2). A solution of compound **4** (2 g, 8 mmol) and aldehyde **3** (1.1 g, 8 mmol) in anhydrous ethanol (45 mL) was refluxed for 5 h. The colorless crystals that formed after cooling of the reaction solution were filtered off, the filtrate after concentration till ~1/3 of volume gave additionally 0.4 g of the product. The yield of compound **2** was 2.5 g (85%). After crystallization from ethanol and then from heptane, m.p. 132—133 °C. Found (%): C, 81.40; H, 6.64; N, 7.45. $C_{25}H_{24}N_2O$. Calculated (%): C, 81.49; H, 6.56; N, 7.60. ^{1}H NMR, δ: 1.29, 1.35 (both s, 3 H each, Me); 2.47 (s, 3 H, Me); 4.23, 4.58 (both d, 1 H each, CH_2Ph, J = 16.4 Hz); 5.97—7.33 (m, 13 H, Ar). Single crystals were obtained by recrystallization from ethanol.

1-Benzyl-3,3,5′,6′-tetramethylspiro[indoline-2,2′-[2*H*]-pyrano[3,2-*b*]pyridinium] iodide (1) was obtained by the N-methylation of the pyridine ring of compound **2** with methyl iodide in THF according to the method described earlier.[14] Found (%): C, 61.19; H, 5.37; I, 25.13; N, 5.42. $C_{26}H_{27}IN_2O$. Calculated (%): C, 61.18; H, 5.33; I, 24.86; N, 5.49. Anhydrous single crystals of **1** were grown from ethanol, the hydrate $\mathbf{1}\cdot H_2O$ was obtained by crystallization from aq. methanol.

X-ray diffraction studies of the salt **1** were performed on an Enraf—Nonius CAD-4 automatic four-circle diffractometer (ω/2θ-scanning, Mo-Kα radiation, 300 K). A yellow single crystal in the shape of parallelepiped sized 0.4×0.4×0.3 mm was used in the experiment. Parameters of the unit cell were determined and refined on 30 reflections found in the range of angles θ from 5 to 10°.

The X-ray diffraction experiments for the single crystals of compounds **2** and $\mathbf{1}\cdot H_2O$ were performed on a Bruker P-4 automatic four-circle diffractometer (θ/2θ-scanning, Mo-Kα radiation, 300 K). For the study of compound **2**, we used a colorless single crystal in the shape of parallelepiped sized 0.15×0.2×0.35 mm, and for $\mathbf{1}\cdot H_2O$, a yellow single crystal sized 0.20×0.25×0.45 mm. It should be noted that the crystals of $\mathbf{1}\cdot H_2O$ were of low quality and underwent slow decomposition on standing. Parameters of the unit cell were determined and refined on 35 reflections found in the range of angles θ from 5 to 10°.

The structures were solved by the direct method. Positions and thermal parameters of nonhydrogen atoms were refined first in isotropic and then in anisotropic approximation by the full-matrix least squares method. Positions of hydrogen atoms in the molecules were found from the differential Fourier syntheses and refined using the riding model. When the oxygen atom of the water molecules in the crystal structure of compound $\mathbf{1}\cdot H_2O$ were refined, the population was also refined along with positional and thermal parameters. Positions of the hydrogen atoms of the water molecules were not found.

The principal crystallographic data and parameters of refinement are given in Table 1. All the calculations were performed using the SHELXTL program package.[23]

Photochemical studies in the crystal state were performed for the thin-layer samples (~10 μm), which were prepared from the mulled single crystals dispersed in Nujol (Aldrich).

A PL-S 9W gas-discharge low pressure mercury lamp producing the UV light in the range 340—390 nm with the maximum at 355 nm was used for the irradiation, as well as a LED with the irradiation 530 nm (60 W) producing a light spot 1.5 cm in diameter.

Absorption spectra were recorded on a Perkin—Elmer Lambda EZ 210 spectrometer. Placement of the samples in the instrument was strictly fixed and the same in each measurement in order to exclude changes in the base line, which depend on the dispersal of the powder when samples are placed differently with respect to the optical axis of the instrument. Changes in the absorption spectra of solutions were recorded on an OceanOptics HR2000 multichannel spectrometer in the automatic scanning mode through the given periods of time. The experimental data that obtained were processed using the Igor Pro 4.0 program.

Results and Discussion

Salts of pyridospiropyran are produced by a two-step synthesis. The condensation of *N*-substituted indoline **4** with pyridinecarbaldehyde **3** leads to the neutral spiropyran **2**, whose N-methylation furnishes pyridinium iodide **1** (Scheme 2).

Molecular and crystal structure of salts 1 and $\mathbf{1}\cdot H_2O$. In the structures of the salts, general configuration of the cation SP^+ (Fig. 1) is the same and similar to the structure of spiropyrans studied earlier.[15—18] The indoline and benzopyran fragments are orthogonal to each other, the angle between the planes {O(1′), C(2′2), C(3′)} and {C(3), C(2′2), N(1)} is 88.7° (89.6°).* The nitrogen atom N(1) has a pyramidal configuration and comes out of the plane of the surrounding carbon atoms by 0.28 Å (0.21 Å). As in all the compounds studied earlier, such a molecular geometry is favorable for the $n_{N(1)}$—σ*[C(2′2)—O(1′)] orbital interactions, which lead to the elongation of the C(2′2)—O(1′) bond to 1.474(4) Å (1.486(5) Å) as compared to the common bond distances, 1.41—1.43 Å, in the

* Here and further parameters are given for compound **1** and in parentheses, for $\mathbf{1}\cdot H_2O$.

Table 1. The crystallographic data and parameters of the X-ray diffraction experiment

Parameter	**1**	**1** · H_2O	**2**
Molecular formula	$C_{26}H_{27}N_2OI$	$C_{26}H_{29}N_2O_2I$	$C_{25}H_{24}N_2O$
M/g mol^{-1}	510.40	542.41	368.46
Crystal system	Monoclinic	Triclinic	Monoclinic
Space group	$P2_1/c$	P-1	$P2_1/n$
a/Å	15.564(3)	8.652(2)	12.890(3)
b/Å	12.738(3)	11.151(2)	9.027(2)
c/Å	12.631(3)	13.886(3)	17.771(4)
α/deg	90.00	103.95(3)	90.00
β/deg	106.78(3)	106.48(3)	98.93(3)
γ/deg	90.00	94.75(3)	90.00
V/Å^3	2397.5(8)	1230.2(4)	2042.7(7)
d_{calc}/g cm^{-3}	1.414	1.427	1.198
Z	4	2	4
μ/mm^{-1}	1.354	1.325	0.073
Region of scanning/deg	1.37—25.01	1.91—25.00	1.82—24.98
Number of measured reflections (R_{int})	4433 (0.0186)	4977 (0.0301)	3983 (0.0227)
Number of reflections with $I > 2\sigma(I)$	4220	4181	2992
Number of refined parameters	275	285	256
GOOF	1.027	0.930	1.071
R_1 ($I > 2\sigma(I)$)	0.0385	0.0550	0.0466
wR_2 (on all ther reflections)	0.1239	0.1547	0.1400

Scheme 2

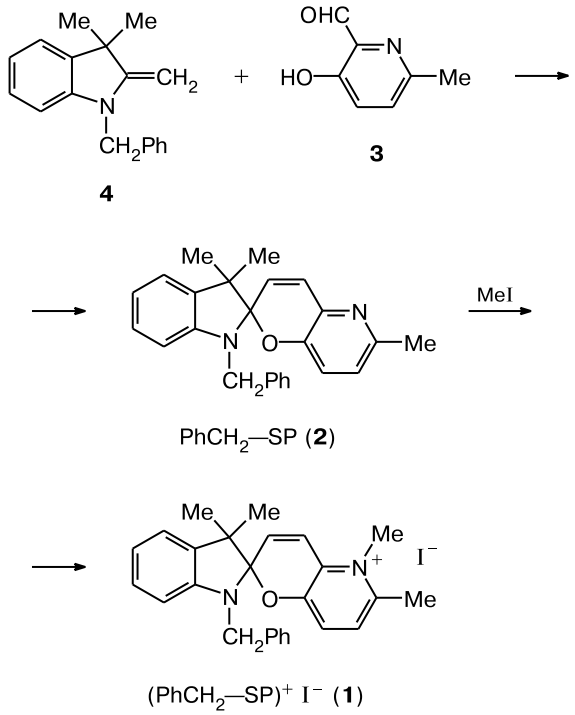

six-membered heterocycles and the shortening of the C(2′2)—N(1) bond to 1.435(5) Å (1.429(6) Å) as compared to the normal C(sp^3)—N(sp^3) bond distances in the five-membered heterocycles 1.47—1.48 Å.[24] The values that obtained coincide within the error limits with the distances of these bonds in cations with other substituents (Me and Pr^i) in the indoline fragment.[15,17]. Thus, the elongation and weakening of the C_{spiro}—O bond makes its photoexcitation cleavage easier.

The turn of the ring in the benzyl substituent with respect to the indoline fragment due to the rotation around the N(1)—C(10) and C(10)—C(11) bonds in the salts is somewhat different, that, obviously, is caused by the packing effects. The torsional angle N(1)—C(10)—C(11)—C(12) is 166.8° (169.4°).

The salt **1**, like the (R—SP)$^+$I$^-$ salts (R = Me and Pr^i),[15,17] crystallizes in the monoclinic crystal system (the

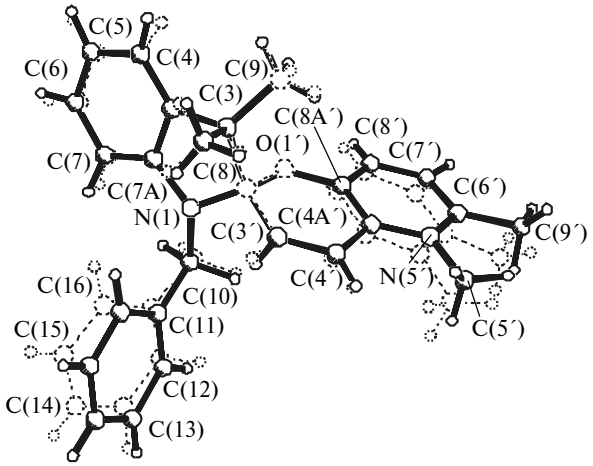

Fig. 1. The cation in the crystal structure **1**, the dashed line shows the cation in the structure of **1** · H_2O.

space group is $P2_1/c$). An increase in the size of substituent in the order Me, Pr^i, and CH_2Ph leads to a natural increase in the parameter *b* of the unit cell (10.959(2), 11.051(3) and 12.738(3) Å, respectively), as well as to a decrease in the calculated density (1.482, 1.439, and 1.414 g cm^{-3}, respectively), that indicate a decrease in the density of packing. The same principle of packing operates for the salts $(R—SP)^+I^-$ (R = Me and Pr^i):[15,17] the cations in the structure are packed in stacks with the indoline fragments around the axis of symmetry 2_1, whereas the pyranopyridinium fragments are turned into the interstack space to the iodine anions; the neighboring stacks are bound between each other by the center of inversion. Unlike the structures studied earlier, whose planes of the indoline fragments of the cation are placed one over another and are almost perpendicular to the axis 2_1 (the angles between the benzene ring of the indoline fragments of the molecules and the axis 2_1 are equal to 71 and 73°), in the crystal structure **1**, the angle between the mean plane of the benzene ring of the indoline fragment and the axis is 29.1° (Fig. 2).

Compound **1** is an ionic one, however, the energy of interactions can be a quality criterion of the characteristic properties of molecular packing in the crystal structure. Calculations of the energy of intermolecular interactions (IMI) in the structure were performed without allowance for the anions in the framework of the atom-atom approximation with the "6-exp" potential.[25] According to the data that obtained, the strongest interactions exist between the molecules bound by the center of inversion: −8.1 and −9.4 kcal mol^{-1}, respectively, for the pairs *C*—*E* and *G*—*E* (see Fig. 2), whereas in the structures $(R—SP)^+I^-$ (R = Me and Pr^i) studied earlier,[15,17] the direction along the *b* axis between pairs of the molecules bound by the screw axis was more pronounced. In this case, the energy of IMI between molecules *E*—*H* and *E*—*B* (see Fig. 2) is considerably lower: −4.2 and −3.3 kcal mol^{-1}, respectively. The energies of IMI (kcal mol^{-1}) with other molecules are of the same order: *D* and *E* (−4.0), *F* and *E* (−3.8), *I* and *E* (−5.4, is somewhat higher due to the overlap of the benzene rings in the substituent). It can be concluded that no pronounced stacks are observed in this salt.

The I^- anions are placed between the pyran (charged) fragments of four cations (see Fig. 2). The shortest distances N(5′)*D*...I(1A) 3.61 Å and N(5′)*A*...I(1A) 3.71 Å indicate a relatively weak interaction of the anion with the positively charged nitrogen atoms of these cations. The anion also forms shortened contacts with two other cations C(4′)*B*...I(1A) 3.88 Å and C(7′)*E*...I(1A) 3.85 Å (the angle I...H—C is 154.9 and 171.4°, respectively).

Crystal structure of the hydrate $\mathbf{1} \cdot H_2O$ (Fig. 3) qualitatively resembles the structure of the salt $(Pr^i—SP)I$ studied earlier:[17] the indoline fragments of cations are perpendicular to the *b* axis and are also packed in stacks, whereas the pyranopyridinium cations are turned into the interstack space, being parallel to each other. The major difference is that in this case cations in stacks are bound by the center of inversion, rather than the screw axis 2_1.

The presence of stacks in this structure was confirmed by calculations of energy of IMI (without allowance for the iodine atoms and water molecules). The energy of IMI between the pairs of cations *C*—*D* and *D*—*C*′ is −8.7 and −10.8 kcal mol^{-1} (see Fig. 3), *i.e.*, the stack forms along the axis. The crystal $\mathbf{1} \cdot H_2O$ significantly differs from the structure of $(Pr^i—SP)I$ obtained earlier[17] by the presence of interactions not only in stacks, but also between them. Thus, the energy of interaction between the pair *B* and *C* is

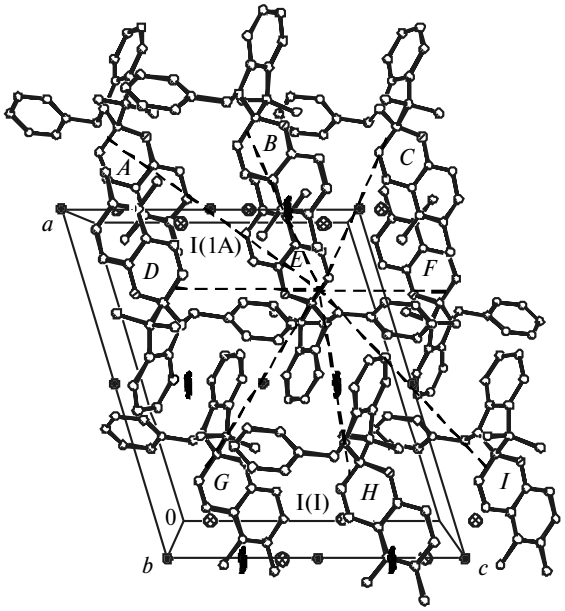

Fig. 2. The projection of the crystal structure **1** on the plane of the cell *ac*. The letters *A*—*I* show cations.

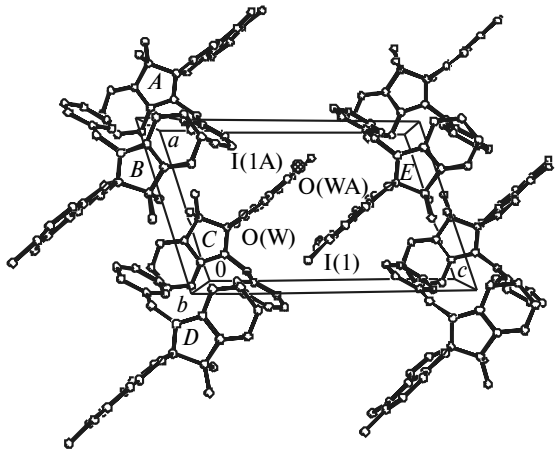

Fig. 3. The projection of the crystal structure $\mathbf{1} \cdot H_2O$ on the plane of the cell *ac*. The letters *A*—*E* show cations. Cations *A*′ and *C*′ are bound with cations *A* and *C* by translation along the axis *b* and are not shown in the Figure.

−7.5 (the short contact C(9)*B*...C(9)*C* is 3.38 Å), the interactions *B*—*D* with the energy −6.6 kcal mol^{-1} (the short contact C(5′)*B*...C(13)*D* is 3.42 Å) and *C*—*E* with the energy −7.2 kcal mol^{-1} (due to the partial overlap of the pyridine rings) should be additionally mentioned. The rest of the interactions are weaker than −3.0 kcal mol^{-1}. The I^- anions in the structure are located between the pyranopyridinium fragments in the interstack space (see Fig. 3), the closest contacts with the cations are: I^-...C(7′) 4.02 Å and I^-...C(4′) 4.14 Å. The shortest distance to the positively charged atom N(5′) of the cation is equal to 3.82 Å.

Since compounds **1** and **1** · H_2O are salts, an ionic type of interaction is mainly responsible for the formation of their crystal structure. Therefore, for the comparison of the crystal structures of these compounds, we selected those structural fragments, where these interactions are the strongest. In the structure **1**, we found the infinite chains ...I^-...N^+...I^-... in the direction of the unit cell axis *b* (Fig. 4). In this chain, the organic cations are arranged according to the "tail-to-tail" principle and are bound between each other by the screw axis. In the structure **1** · H_2O, the chains ....I^-....N^+....I^-.... are also observed (Fig. 5), but in this case cations in the chain are bound between each other by translations along the *a* axis and the distance N^+—I^-—N^+ is longer than in the first case.

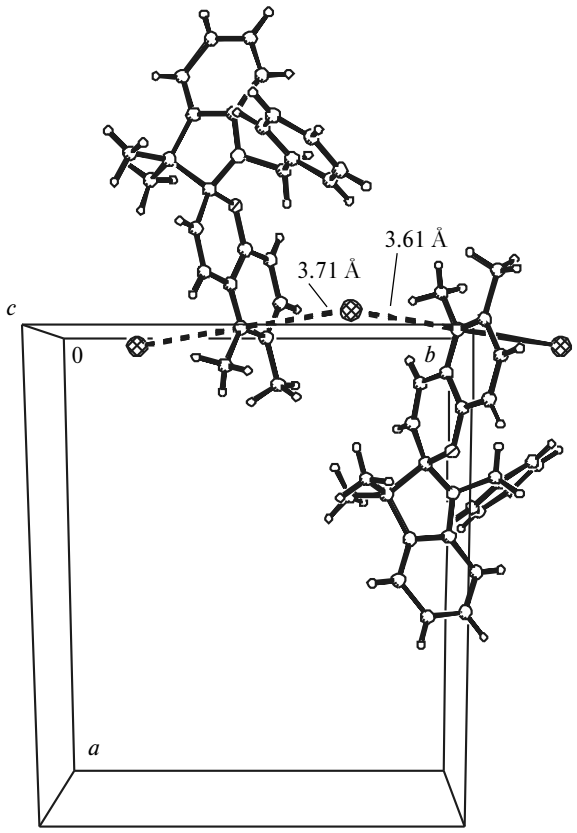

Fig. 4. The fragment of the crystal structure **1**. The dashed lines show the intermolecular contacts.

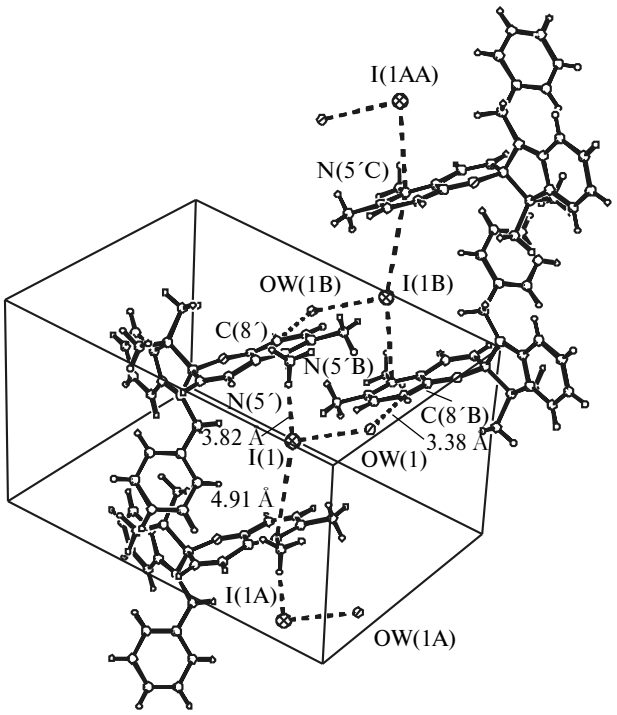

Fig. 5. The fragment of the crystal structure **1** · H_2O. The dashed lines show the intermolecular contacts.

The water in the structure **1** · H_2O has weak van der Waals interactions with I^- anion O(W)...I(1) 3.64 Å (the radius for O is 1.40 Å, for I 2.15 Å).[26] The water molecule also has a weak contact with the pyridine part of the cation O(W)...C(8′) 3.37 Å. The water in the structure is weakly bound, that, by all accounts, is the reason for the high thermal parameters, and its positions are populated by 80%. Probably, the loss of water is responsible for decomposition of the crystals on storage. Despite that water in the structure is weakly bound, it significantly affected formation of the crystal **1** · H_2O. The crystal structure of anhydrous compound **1** differs from the structure of the hydrate, but in this case, a single formal unit in the crystals has virtually the same volume (599.4 and 615.1 Å^3 for **1** and **1** · H_2O, respectively).

Molecular and crystal structure of neutral spiropyran 2. Molecular structure of spiropyran **2** differs little from the structures of the salt forms. In the neutral compound, likewise in the salts, the C(2′2)—O(1′) bond is elongated to 1.471(2) Å, whereas the C(2′2)—N(1) bond is shortened to 1.449(3) Å. The $n_{N(1)}$—σ*[C(2′2)—O(1′)] interactions tend to strengthen in the order of compounds **2**, **1**, and **1** · H_2O.

Like the neutral spiropyran[15] Me—SP, compound **2** crystallizes in the monoclinic crystal system, the space group is $P2_1/n$. An increase in the size of the molecule **2** leads to the natural growth in the size of the unit cell (1568(1) and 2042.7(7) Å^3 for Me—SP and **2**, respectively). Unlike the salts, molecules in the crystal structure of

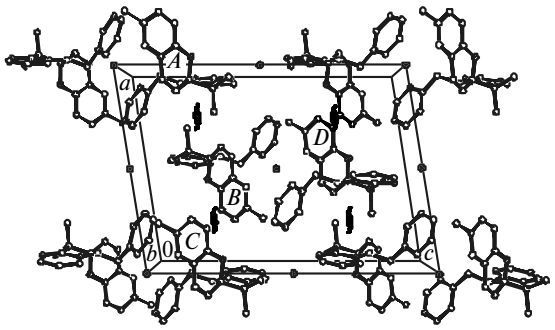

Fig. 6. The projection of the crystal structure **2** on the plane of the cell *ac*. The letters *A*—*D* show the molecules.

the neutral compound **2** are packed along the axis 2_1 with the pyranopyridine fragments (Fig. 6). According to the calculations of the energy of IMI by the known method,[25] the packing has no clearly cut stacks. Thus, the energies of IMI between the molecules bound by the screw axis are −9.2 and −7.0 kcal mol^{-1} (for the pairs *A*—*B* and *B*—*C*, respectively, see Fig. 6). For the molecules bound by the center of inversion, the energies of IMI are −5.1 (*B* and *D*) and −11.3 kcal mol^{-1} (*D* and *B*′). The structure has no shortened interactions, the shortest intermolecular contacts exceed 3.46 Å.

Photochemistry of neutral and salt forms of spiropyrans. Photochromic properties of the neutral compound **2** do not differ from the properties of the earlier studied R—SP (R = Me and Pr^i). The absorption spectrum of **2** in ethanol has a band with λ_{max} = 310 nm. Steady irradiation of the solution with the UV light (330 nm) leads to its coloring and formation of a short-lived open form with the absorption maximum at 580 nm and the rate constant of dark cyclization $k = 6.16(2) \cdot 10^{-2}$ s^{-1} (18 °C).

In the series of R—SP (R = Me, Pr^i, CH_2Ph), the absorption maximum of the open form is somewhat displaced to the long-wave region of the spectrum, whereas the dark bleaching constant values are close; the lifetime of the MC-form is ≤1 min. The open form was not registered upon the steady irradiation in the nonpolar solvent (hexane). Such a difference in the stability of the open form in polar and nonpolar solvents is explained not only by polarity of the solvent, but also, probably, by the formation of hydrogen bonds of the alcohol molecules with the nitrogen atom of the pyridine ring of the molecule. Crystals of the spiropyran **2** are not photochromic upon the steady irradiation.

Unlike the neutral forms, their salts form an MC-form in solutions of polar solvents, whose lifetime lasts for hours. When irradiated with the UV light (355 nm), the solution in ethanol acquires a bright pink color (a wide maximum at 545—560 nm), whereas a solution in chloroform becomes dark violet (λ_{max} = 593 nm). Kinetics of the dark bleaching of solutions is described by a monoexponential equation (Table 2).

Table 2. Spectral characteristics and constants of the dark bleaching of the salt **1** in solutions

Solvent	λ_{max}/nm (ε_{max}/L mol^{-1} cm^{-1})		$k \cdot 10^5$/s^{-1}
	SP	MC	
$CHCl_3$	355 (17950)	565 (sh), 593	11.6(2)
EtOH	350 (13200)	545 (sh), 580	3.1(1)

The packing of molecules in the crystals of salts **1** and **1** · H_2O provides a free volume enough for the photochromic transformations. The long-lived MC-forms are formed in the irradiated crystals of iodides, like in solutions, whose stability is secured by the electron-withdrawing pyridinium ring.

The changes in the absorption spectra of polycrystals of the salt **1** upon irradiation with the UV light (355 nm) are shown in Fig. 7. A band in the region 550—650 nm characteristic of absorption of the MC-form appears in the spectra, with the simultaneous decrease in the intensity of the band of the cyclic form. Similar behavior is observed for the crystals **1** · H_2O and the spectra that recorded for both the starting and the colored forms do not differ from the corresponding spectra in the case of compound **1**. Like in solutions, a shift of the absorption maximum of the open form to the long-wave region is observed in the series of (R—SP)$^+$I$^-$ (R = Me, Pr^i, CH_2Ph) (Table 3).

After exposure to the visible light (530 nm), the spectrum returns to the starting shape. The open form slowly returns to the cyclic one at room temperature under dark conditions. Kinetics of the dark bleaching of the salts is described by the biexponential dependence (Fig. 8). For the hydrate **1** · H_2O, the contribution of the fast reaction is noticeably larger than for **1**, with the contribution of the fast reaction increasing in the order (Me—SP)$^+$I$^-$, (Pr^i—SP)$^+$I$^-$, **1**, **1** · H_2O (see Table 3). If kinetics of

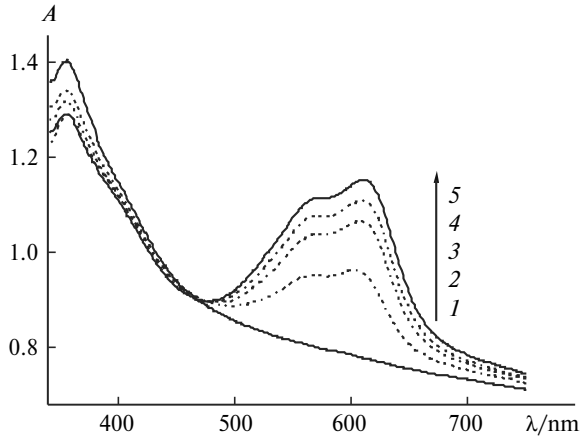

Fig. 7. The changes in the absorption spectra of the polycrystals **1** with time upon irradiation with the UV light (355 nm): t = 0 (*1*), 10 (*2*), 30 (*3*), 60 (*4*), and 120 s (*5*).

Table 3. Spectral and kinetic characteristics and calculated densities of the crystal salts $(R—SP)^+I^-$

Compound	d_{calc}/g cm^{-3}	λ_{max}/nm		$k_1 \cdot 10^4$	$k_2 \cdot 10^6$	A_1/A_2
		SP	MC	s^{-1}		
(Me—SP)I *	1.482	355	560, 595	—	2.6	—
(Pr^i—SP)I *	1.439	352	560, 597	1.6	11.0	0.22
1	1.414	355	560, 610	3.3(7)	6.4(5)	0.54(4)
1 · H_2O	1.427	360	560, 620	1.5(1)	3.1(2)	1.09(2)

* Photochemical studies of the salts have been performed earlier.[6,15]

bleaching is monoexponential in $(Me—SP)^+I^-$,[14,15] the biexponential kinetics[6] corresponds to the salt $(Pr^i—SP)^+I^-$ [6] with a low contribution of the fast reaction. For the salt **1**, the ratio A_1/A_2 is already 0.54(4), whereas for the hydrate **1** · H_2O it reaches 1.09(2). The data that obtained agree with the decrease in the density of packing in this series of spiropyrans described by us above (see Table 3).

In conclusion, the positively charged pyridinium ring in the salts is an important factor for the photochromic transformations to take place not only in solutions, but also in the crystal state: the positively charged ring stabilizes the open form due to its electron-withdrawing effect.

Molecular geometry in both the neutral compounds and the salts favors the $n_{N(1)}$—σ*[C(2′2)—O(1′)] orbital interactions, which lead to the elongation of the C(2′2)—O(1′) bond and shortening of the C(2′2)—N(1) bond as compared to the normal bond distances in heterocycles. The tendency to the strengthening of the *n*—σ*-interactions is observed in the series of studied compounds **2**, **1**, **1** · H_2O.

The in detail analysis of intermolecular contacts showed that for the salts $(R—SP)^+I^-$ (R = Me, Pr^i), **1**, **1** · H_2O, the same principle of packing operates: in the crystal their indoline fragments are bound by more strong interactions, whereas the pyranopyridine fragments together with the I^- ions are placed between stacks and have more loose packing. Such a structure of the salts provides a possibility of photochromic transformations of the cation in crystals.

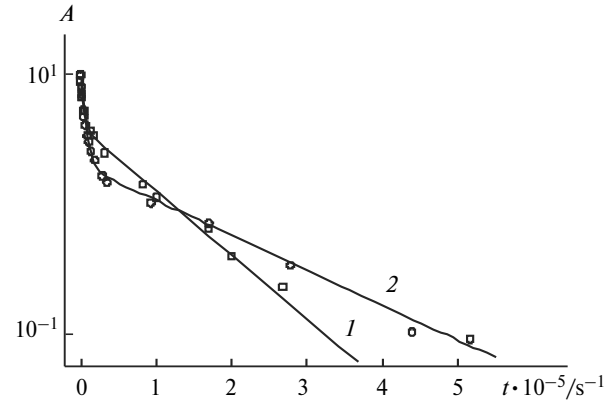

Fig. 8. Kinetics of the dark bleaching of the polycrystals **1** (*1*) and **1** · H_2O (*2*). The experimental dots are normalized on the value of initial absorption. The solid lines are the approximation of the biexponential function $A(t) = A_1\exp(-k_1t) + A_2\exp(-k_2t)$ fall. The ordinate axis has a logarithmic scale.

This work was financially supported by the Presidium of Russian Academy of Sciences (Program of Basic Research of the RAS No. 18 "Development of Methods for Preparation of Chemical Compounds and Creation of New Materials", Subprogram "Polyfunctional Materials for Molecular Electronics").

References

1. O. Sato, J. Tao, Y.-Z. Zhang, *Angew. Chem., Int. Ed.*, 2007, **46**, 2152.
2. Y. Einaga, *J. Photochem. Photobiol. C: Photochem. Rev.*, 2006, **7**, 69.
3. S. M. Aldoshn, *Izv. Akad. Nauk, Ser. Khim.*, 2008, 704 [*Russ. Chem. Bull., Int. Ed.*], 2008, **57**, 718.
4. W. Fujita, K. Awaga, T. Yokoyama, *Appl. Clay Sci.*, 1999, **15**, 281.
5. H. Shimizu, M. Okubo, A. Nakamoto, M. Enomoto, N. Kojima, *Inorg. Chem.*, 2006, **45**, 10240.
6. S. Bénard, E. Rivière, P. Yu, K. Nakatani, J. F. Delouis, *Chem. Mater.*, 2001, **13**, 159.
7. S. M. Aldoshin, N. A. Sanina, V. I. Minkin, N. A. Voloshin, V. N. Ikorskii, V. I. Ovcharenko, V. A. Smirnov, N. K. Nagaeva, *J. Mol. Struct.*, 2007, **826**, 69.
8. S. M. Aldoshin, N. A. Sanina, V. A. Nadtochenko, E. A. Yurieva, V. I. Minkin, N. A. Voloshin, V. N. Ikorskii, V. I. Ovcharenko, *Izv. Akad. Nauk, Ser. Khim.*, 2007, 1055 [*Russ. Chem. Bull., Int. Ed.*, 2007, **56**, 1095].
9. I. Kashima, M. Okubo, Y. Ono, M. Itoi, N. Kida, M. Hikita, M. Enomoto, N. Kojima, *Synth. Met.*, 2005, **155**, 703.
10. N. Kida, M. Hikita, I. Kashima, M. Okubo, M. Itoi, M. Enomoto, K. Kato, M. Takata, N. Kojima, *J. Am. Chem. Soc.*, 2009, **131**, 212.
11. N. Kida, M. Hikita, I. Kashima, M. Enomoto, M. Itoi, N. Kojima, *Polyhedron*, 2009, **28**, 1694.
12. S. Bénard, A. Léaustic, E. Rivière, P. Yu, R. Clément, *Chem. Mater.*, 2001, **13**, 3709.
13. M. Okubo, M. Enomoto, N. Kojima, *Synth. Met.*, 2005, **152**, 461.
14. S. Bénard, P. Yu, *Adv. Mater.*, 2000, **12**, 48.

15. S. M. Aldoshin, L. A. Nikonova, V. A. Smirnov, G. V. Shilov, N. K. Nagaeva, *J. Mol. Struct.*, 2005, **750**, 158.
16. S. M. Aldoshin, L. A. Nikonova, V. A. Smirnov, G. V. Shilov, N. K. Nagaeva, *Izv. Akad. Nauk, Ser. Khim.*, 2005, 2050 [*Russ. Chem. Bull., Int. Ed.*, 2005, **54**, 2113].
17. S. M. Aldoshin, L. A. Nikonova, G. V. Shilov, E. A. Bikanina, N. K. Artemova, V. A. Smirnov, *J. Mol. Struct.*, 2006, **794**, 103.
18. V. V. Tkachev, S. M. Aldoshin, N. A. Sanina, B. S. Luk´yanov, V. I. Minkin, A. N. Utenyshev, K. N. Khalanskii, Yu. S. Alekseenko, *Khim. Geterotsikl. Soedin.*, 2007, 690 [*Chem. Heterocycl. Compd.* (*Engl. Transl.*), 2007, **43**, 576].
19. P. Naumov, P. Yu, K. Sakurai, *J. Phys. Chem. A*, 2008, **112**, 5810.
20. N. Clauson-Kaas, M. Meister, *Acta Chem. Scand.*, 1967, **21**, 1104.
21. C. D. Weis, *J. Heterocycl. Chem.*, 1978, **15**, 29.
22. C. H. Tilford, *J. Med. Chem.*, 1971, **14**, 1020.
23. G. M. Sheldrick, *SHELXTL v. 6.14, Structure Determination Software Suite*, Bruker AXS, Madison (Wisconsin, USA), 2000.
24. F. H. Allen, O. Kennard, D. G. Watson, L. Brammer, A. G. Orpen, R. Taylor, *J. Chem. Soc., Perkin Trans. 2*, 1987, S1.
25. G. V. Timofeeva, N. Yu. Chernikova, P. M. Zorkii, *Usp. Khim.*, 1980, **49**, 966 [*Russ. Chem. Rev.* (*Engl. Transl.*), 1980, **49**, 509.

Received March 4, 2011;
in revised form June 14, 2011